Molecular Cell, Vol. 15, 991–997, September 24, 2004, Copyright ©2004 by Cell Press

Conformational Switching by the Scaffolding Protein D Directs the Assembly of Bacteriophage ϕX174

Marc C. Morais,[1,3] Megan Fisher,[1,3] Shuji Kanamaru,[1,4] Laralynne Przybyla,[1] John Burgner,[1] Bentley A. Fane,[2] and Michael G. Rossmann[1,*]
[1]Department of Biological Sciences
Purdue University
915 West State Street
West Lafayette, Indiana 47907
[2]Department of Veterinary Science and Microbiology
University of Arizona
Building 90
Room 201
Tucson, Arizona 85721

Summary

The three-dimensional structure of bacteriophage ϕX174 external scaffolding protein D, prior to its interaction with other structural proteins, has been determined to 3.3 Å by X-ray crystallography. The crystals belong to space group $P4_12_12$ with a dimer in the asymmetric unit that closely resembles asymmetric dimers observed in the ϕX174 procapsid structure. Furthermore, application of the crystallographic 4_1 symmetry operation to one of these dimers generates a tetramer similar to the tetramer in the icosahedral asymmetric unit of the procapsid. These data suggest that both dimers and tetramers of the D protein are true morphogenetic intermediates and can form independently of other proteins involved in procapsid morphogenesis. The crystal structure of the D scaffolding protein thus represents the state of the polypeptide prior to procapsid assembly. Hence, comparison with the procapsid structure provides a rare opportunity to follow the conformational switching events necessary for the construction of complex macromolecular assemblies.

Introduction

The assembly of complex macromolecules typically proceeds along well-ordered morphogenetic pathways. Although macromolecular assembly is a fundamental biological process, assembly pathways have been characterized most thoroughly in viral systems (Casjens and Hendrix, 1988; King et al., 1980). A generally accepted model for virion morphogenesis invokes the notion of "conformational switching" (Berget, 1985; Caspar, 1980; King et al., 1980; Wood and Conley, 1979). In this model, a nucleation event initiates assembly. In each subsequent step, a protein that binds to the growing structure undergoes a conformational change, creating a new binding site for the next protein. Although scaffolding proteins are not found in mature virions, capsid assembly frequently requires their participation to nucleate the reaction and ensure temporal fidelity (Casjens and Hendrix, 1988; Fane and Prevelige, 2003; King and Casjens, 1974; Ray and Murialdo, 1975; Showe and Black, 1973). The absence of scaffolding proteins results in either arrested assembly or aberrant particle formation. Thus, scaffolding proteins function as higher order equivalents of molecular chaperones, regulating quaternary structure in the same way that chaperones regulate tertiary structure (Dokland, 1999).

Bacteriophage systems, in which biochemical, genetic, and structural data can be correlated, have been particularly informative in the study of scaffolding-directed assembly (Dokland et al., 1997, 1999; Fane and Prevelige, 2003; Hayashi et al., 1988; Morais et al., 2003; Sun et al., 2000; Thuman-Commike et al., 2000). Bacteriophage ϕX174 utilizes two scaffolding proteins for capsid morphogenesis, whereas most larger double-stranded DNA (dsDNA) viruses employ only one. The internal scaffolding (B) and external scaffolding (D) proteins perform most or all the functions associated with single scaffolding proteins found in other viral systems.

The first detectable ϕX174 assembly intermediates are the 9S and 6S particles, pentamers of the F viral coat and G spike proteins, respectively (Figure 1A). Five copies of the internal scaffolding protein B bind to the coat protein pentamer to assemble 12S particles. Twenty external D scaffolding proteins then bind to 12S particles to form 18S particles, thereby inducing conformational changes that enable the 18S pentamers to associate into icosahedral, "open" procapsids (Fane and Hayashi, 1991; Fujisawa and Hayashi, 1977; Siden and Hayashi, 1974; Tonegawa and Hayashi, 1970). Procapsids have a 360 Å diameter with their 5-fold vertices adorned by pentamers of G spike proteins. The crystal structure of an off-pathway "closed" procapsid (Dokland et al., 1997, 1999) has been determined. The capsid and major spike proteins in the closed procapsid have a similar structure as that observed in the mature virus. The open procapsid, which most likely represents the true morphogenetic intermediate, has been examined by cryo-electron microcopy (cryo-EM) (Dokland et al., 1999). In contrast to the closed procapsid, the open procapsid has 30 Å pores along the 3-fold icosahedral axes and 10 Å gaps between the F capsid pentamers. In the closed procapsid, these pores are occluded by the α4 helices of 3-fold related F capsid proteins. DNA packaging and maturation brings about a radial collapse of the procapsid, resulting in the closure of the gaps surrounding the F pentamers and movement of the α4 helices into the pores at the 3-fold axes.

The procapsid icosahedral asymmetric unit contains four D proteins (D_1, D_2, D_3, and D_4), organized into 120 "asymmetric dimers" ("D_1D_2" or "D_3D_4") over the surface of the particle (Figure 1B). Despite some structural differences, the four monomers (D_1–D_4) share a common core. Overall, the protein is best described as having seven major helices separated by six short loop regions (Figure 1C). Loop 5 is highly polymorphic, forming β structure in some subunits (Dokland, 1999; Dokland et al., 1997,

*Correspondence: mgr@indiana.bio.purdue.edu
[3]These authors contributed equally to this work.
[4]Present address: Department of Life Science, Bioscience and Biotechnology, Tokyo Institute of Technology, 4259 Nagatsuta, Midoriku, Yokohama 226-8501, Japan.

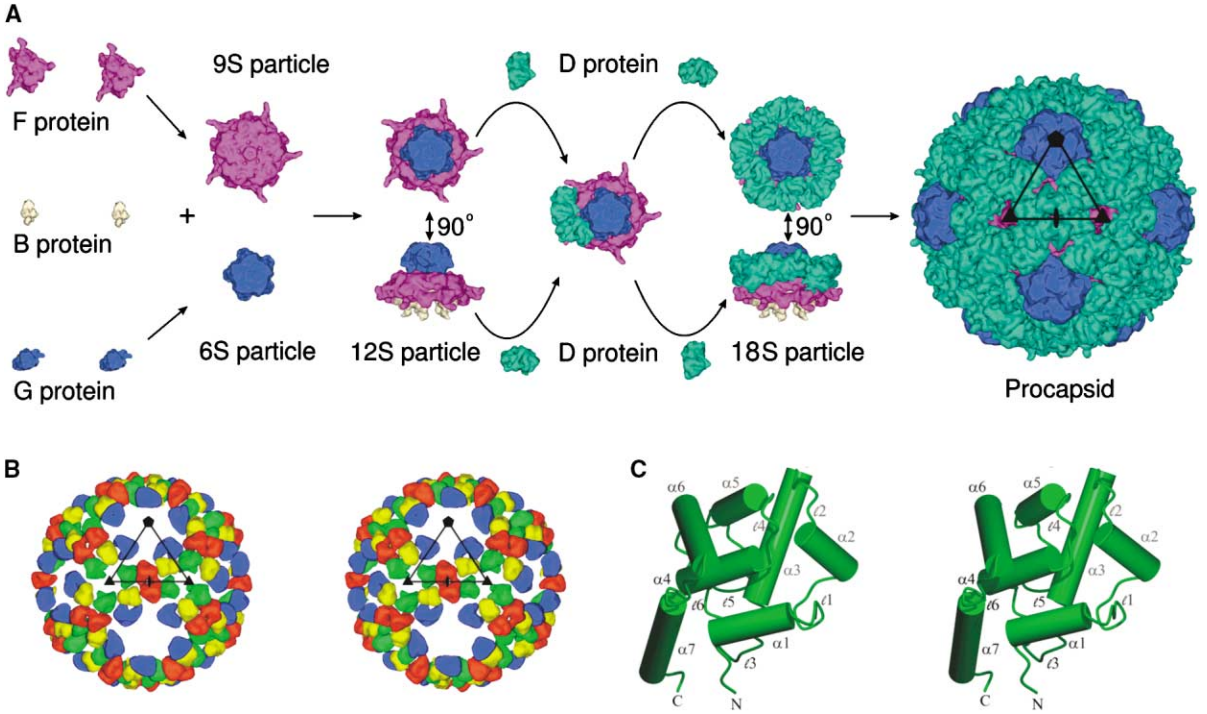

Figure 1. The Structure and Organization of the Scaffolding Protein D

(A) Procapsid assembly in ϕX174. The first morphogenetic intermediates in the assembly pathway are the 9S and 6S particles, pentamers of the F capsid (shown in pink) and G spike proteins (shown in blue), respectively. Five copies of the internal scaffolding protein B (shown in white) promote the association of 9S and 6S particles to form 12S intermediates. Asymmetric dimers of the external D scaffolding protein (shown in green) direct the assembly of pentameric 12S intermediates into the procapsid shell. The icosahedral asymmetric unit of the procapsid is indicated in black.

(B) Stereo diagram showing the lattice of the D protein in the procapsid. There are four copies of the external D scaffolding protein (D_1, blue; D_2, yellow; D_3, red; and D_4, green) in the icoahedral asymmetric unit of the procapsid. The icosahedral asymmetric unit and its associated symmetry elements are shown in black.

(C) Stereo diagram of monomer D_4 of the procapsid shown diagrammatically with cylinders for helices. Helices and loops are labeled using Greek and cursive fonts respectively.

1999). The monomers within each asymmetric dimer are related by a 51° rotation. Whereas D_1 and D_3 are quite similar in structure (with an rms deviation of 1.4 Å between equivalent C_α atoms), they differ substantially from the structures of D_2 and D_4 (Table 1).

Conformational changes in protein structure are invoked in numerous hypotheses regarding molecular mechanisms in biology, but only in a few cases is the precise nature of these changes known. Here, we present the crystallographic structure of the ϕX174 external scaffolding protein prior to conformational changes induced by other structural proteins. Combining these results with the previously reported biochemical and structural data for ϕX174 (Burch and Fane, 2003; Dok-

Table 1. Differences between Equivalent C_α Atoms between D Protein Monomers

D Protein Pair	Rms Differences (Å), All Residues[a]	Rms Differences (Å), Equivalent Residues[a]	Rotational Relationship (°)
D1-D3	1.4	0.4	115.3
D2-D4	7.5	0.3	111.6
D1-D2	4.1	0.4	52.8
D3-D4	8.8	0.4	49.3
D1-D4	8.8	0.5	165.6
D2-D3	7.5	0.4	65.0
DA-DB	4.2	0.4	115.3
DA-D1	1.3	0.7	NA
DA-D3	1.0	0.6	NA
DB-D2	3.6	0.6	NA
DB-D4	5.1	0.5	NA

[a]The Rms difference is taken over "all residues" in the protein, or only the "equivalent residues" in the structurally conserved core.

land et al., 1997; Hayashi et al., 1988; A. Uchiyama and B.A.F., unpublished data) illuminates the conformational changes that occur during the assembly of a virus.

Results

The oligomeric state of the D protein was characterized by gel filtration and sedimentation experiments (see Experimental Procedures). Gel filtration showed that the protein had formed tetramers in solution, consistent with previous results (Farber, 1976; Tonegawa and Hayashi, 1970). Sedimentation velocity and equilibrium experiments indicated an equilibrium between dimers and tetramers.

The X-ray crystallographic structure of the D scaffolding protein was determined to 3.3 Å resolution by molecular replacement using D protein models obtained from the procapsid crystal structure (Dokland, 1999). Since four structurally distinct copies of protein D (D_1–D_4) are in the procapsid's icosahedral asymmetric unit, there was no way of knowing a priori which conformer would correspond most closely to the crystallized D protein. Therefore, each of the four conformationally different copies of the D protein was used as an initial search model. The best result was obtained using monomer D_3. Assuming a Matthews coefficient of 2.5 Å^3/Da, four monomers were expected in the asymmetric unit. It was, therefore, surprising that only two copies, D_A and D_B, were found in the asymmetric unit, corresponding to a Matthews coefficient of 5.0 Å^3/Da and a solvent content greater than 70%.

The structure of D_A is closest to the structures of D_1 and D_3, whereas the structure of D_B is closest to the structures of D_2 and D_4 (Figure 2A; Table 1). Furthermore, the angle between D_A and D_B is 51°, very similar to the angle between D_1 and D_2 and between D_3 and D_4. Thus, the D_AD_B dimer in the crystallographic asymmetric unit is similar to the asymmetric dimers D_1D_2 and D_3D_4 suggested as assembly intermediates of the procapsid (Dokland et al., 1997). In addition, the 4_1 screw relationship between neighboring asymmetric units in the D_AD_B crystal is approximately that found between the two asymmetric dimers in the procapsid (Figures 2B and 2C). Whereas the rotation is 90° and the translation is 31.8 Å between the asymmetric dimer D_AD_B and the 4_1 symmetry-related asymmetric dimer $D_A'D_B'$ in the crystal, the rotation is 114° and the translation is 40 Å between the D_1D_2 and the D_3D_4 dimers in the procapsid. There are no other symmetry contacts between the D molecules in the crystal that resemble other D-D contacts in the procapsid. For instance, there are 2-fold symmetry operators in the D_AD_B crystal structure, but these have no relation to the 2-fold axes in the icosahedral procapsid.

In both the D_AD_B crystal structure and in the procapsid structure, the *inter*dimer interface resembles the *intra*dimer interface. In the procapsid the D_2D_3 interface is similar to the D_1D_2 interface (Figure 3A), and in the D_AD_B crystal structure the D_BD_A' interface is similar to the D_AD_B interface (Figure 3B). The difference between the inter- and intradimer interfaces is determined by whether helix α3 is straight or kinked. Specifically, the interface within an asymmetric dimer involves a kinked helix α3 in D_A, D_1, or D_3, whereas the interface between asymmetric dimers involves a straight helix α3 in D_B or D_2, respectively. Therefore, the crystal structure can be described approximately as having an 8-fold screw helix with an average rotation of 45° (alternate rotations of 51° and 39°) and translation of 15.9 Å between individual D molecules. The same is true for the procapsid, except the oligomerization extends only over four D molecules (Figures 2B and 2C). Indeed, if there were no conformational switching and two D molecules were to bind with a 45° rotation, then an infinite 8-fold screw helix would result (Caspar and Klug, 1962). The oligomeric form of D protein in solution suggests that the basic morphogenetic building block is a tetramer composed of two consecutive asymmetric dimers arranged as found both in the D_AD_B crystal structure and the procapsid. Conformational switching, when two asymmetric dimers associate to form a tetramer, presumably inhibits further oligomerization (see below).

In each monomer of the tetramer, there is a structurally conserved core consisting of approximately 50% of the sequence (residues 27–60, 73–98, and 116–128). The cores superimpose with an rms deviation of less than 2.5 Å. Large differences are localized to four regions: (1) the kink in helix α3, which also determines the position of loop 3; (2) the degree of order and position of helix α7; (3) the orientation of helix α1 relative to the core; and (4) the degree of order and position of loop 5. In the procapsid, all of these regions are component parts of intermolecular contacts between D and F, D and G, or D and neighboring D proteins. These differences, discussed in turn below, are most likely critical for morphogenesis, providing unique binding surfaces for directing assembly (Burch and Fane, 2000, 2003; Dokland et al., 1999; A. Uchiyama and B.A.F., unpublished data).

Discussion

The α3 Helix in the D Protein

The two D molecules within the asymmetric dimer differ especially in the kinking of helix α3, suggesting the presence of a conformational switch in the dimerization process. The kink in helix α3 can only be accommodated by a glycine residue at position 61, since the torsion angles necessary to form the kink occupy a forbidden region of the Ramachandran plot. The importance of this glycine has been demonstrated in vivo by site-directed mutagenesis (Burch and Fane, 2003). Substitutions for this glycine result in dominant lethal phenotypes, which indicates that the mutant protein is still capable of interacting with wild-type protein in coinfected cells. However, this interaction sequesters the wild-type protein, thus preventing the formation of procapsids.

If there were no conformational switch in the formation of an asymmetric dimer, then helix α3 in D_2 would be kinked as it is in D_1, allowing D_3 to form an interface with D_2 identical to that between D_2 and D_1, creating a further 51° rotation (alternatively, all the α3 helices might have been straight). This process could continue indefinitely creating a helix, but it does not because of the conforma-

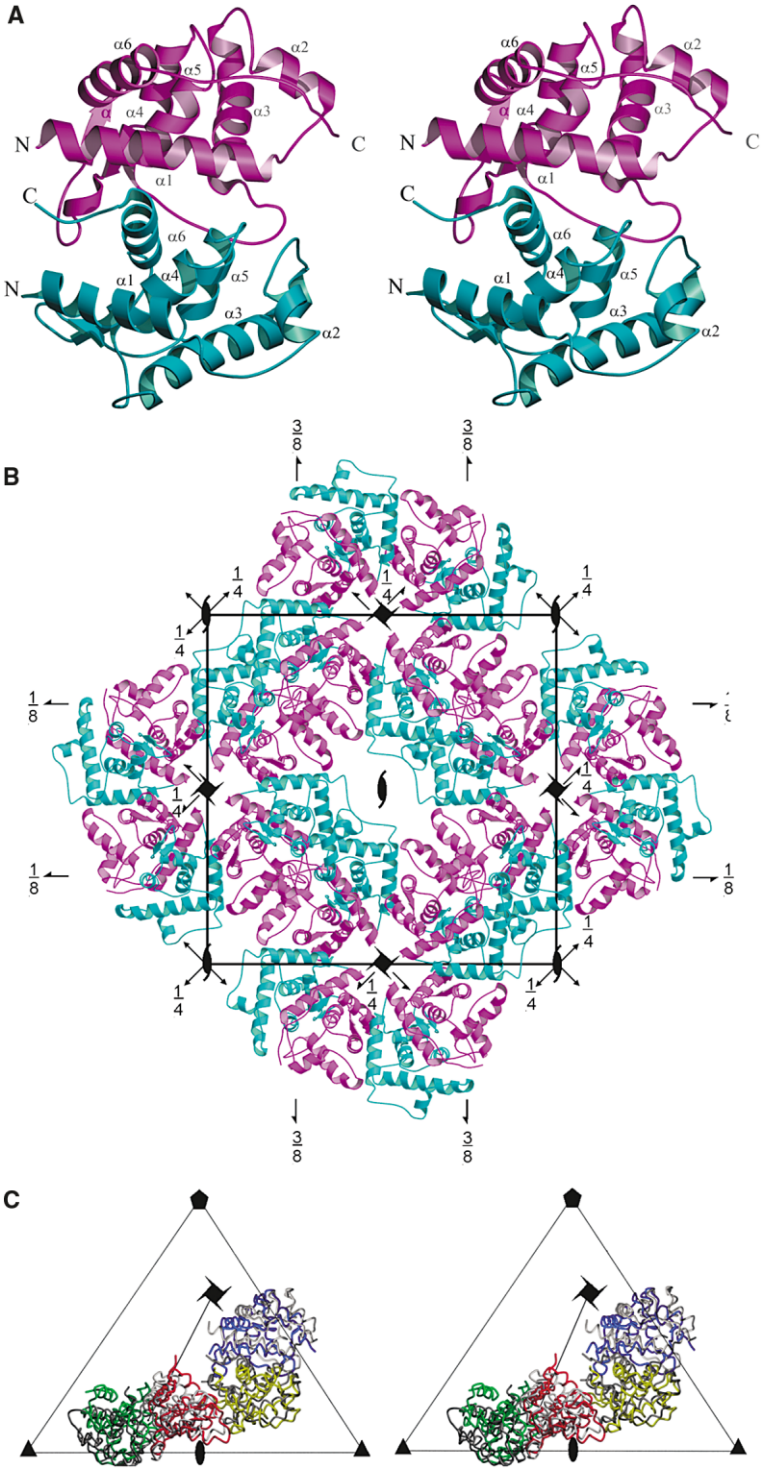

Figure 2. The Structure of the D Protein Prior to Procapsid Assembly

(A) Stereo diagram showing one asymmetric dimer, with D_A shown in magenta and D_B in cyan.

(B) Arrangement of the D protein in the crystal lattice, viewed down the 4_1 axis. Unit cell boundaries and symmetry elements are shown in black.

(C) Stereo diagram showing D protein tetramers superimposed. D_1, D_2, D_3, and D_4 from the procapsid icosahedral asymmetric unit are shown in blue, yellow, red, and green, respectively. D_A and D_A' from the $P4_12_12$ crystal structure are shown in light gray, D_B and D_B' in dark gray. The asymmetric dimer $D_A'D_B'$ was generated via one application of the crystallographic 4_1 operator to the D_AD_B dimer. The procapsid icosahedral symmetry elements and the crystallographic 4_1 axis are shown in black.

tional changes in D_2. As a result, the D_2-D_3 binding surface (1512.54 Å^2) is not as extensive as the D_1-D_2 binding surface (2270.48 Å^2), suggesting that the asymmetric dimers are stable assembly intermediates. However, these dimers are still able to assemble with each other via the decreased binding surface, inducing conformational changes on each other that inhibit further polymerization at either end of the tetramer. Binding of the tetramer to the 12S particle induces mutual conformational changes necessary for procapsid formation. During crystallization, there is a separation of the asymmetric dimers, reversing the conformational switch that occurred in tetramer formation and, therefore, creating the infinite 8_1 helices in the crystal. Hence, the D_AD_B dimer in the crystal structure probably represents the structure of the asymmetric dimer prior to tetramerization.

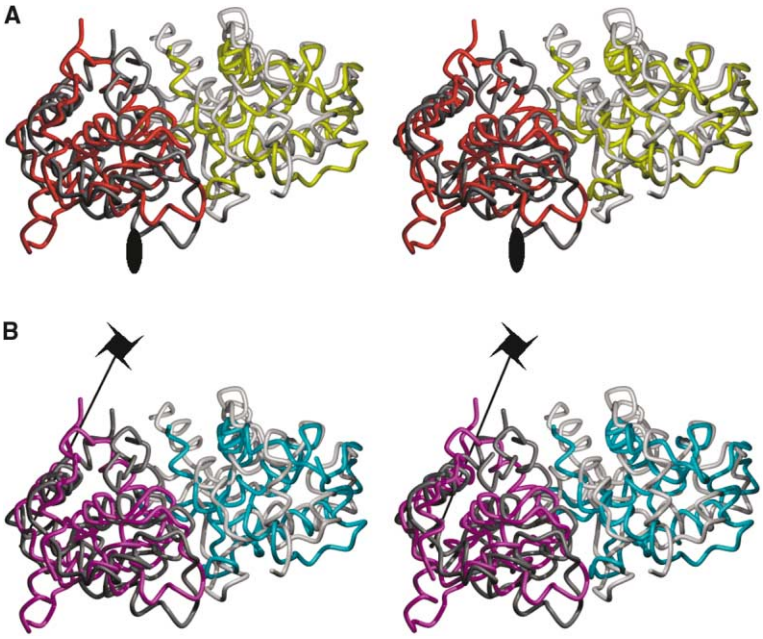

Figure 3. Stereo Diagram Showing the Superposition of D Protein Dimers

(A) Superposition of D_1D_2 onto D_2D_3. D_1 and D_2 are shown in light and dark gray, respectively. D_2 and D_3 are colored as in previous figures, with D_2 in yellow and D_3 in red. Icosahedral 2-fold symmetry axes are indicated as black ellipses.

(B) Superposition of D_AD_B onto D_BD_A'. The rotated/translated copies of D_A and D_B are shown in light and dark gray, respectively. D_B and D_A' are shown in cyan and magenta, respectively. The crystallographic 4_1 axis is indicated in black.

Helix α7 in the D Protein

The C termini of the D proteins in the closed procapsid are structurally diverse. In D_1, D_2, and D_3, the terminus is solvent exposed and either partly or completely disordered. In D_4, however, it is ordered all the way to the end of the protein, forming the long, straight helix α7, and is responsible for most of the interactions between the external D scaffolding proteins and the F capsid protein, as observed in the closed procapsid. In the D_B subunit, there are five ordered N-terminal residues in helix α7. This suggests that helix α7 becomes ordered only when these residues contact the capsid protein F, thereby locking the D tetramers onto the 12S particle. Chimeric ϕX174 external scaffolding proteins in which the wild-type helix α7 has been replaced with the homologous helix from another *Microviridae* bacteriophage assemble structural proteins into defective procapsids that cannot package DNA. Presumably, the resulting external lattice of mutant D proteins cannot interact properly with the packaging machinery (Burch and Fane, 2000, 2003).

Helix α1 in the D Protein

The amino-terminal 23 residues of protein D form the amphipathic helix α1. In the D_4 subunit of the closed procapsid, this helix is bent at Gln22 by 100° relative to the orientation found in the D_1, D_2, and D_3 subunits. In D_B, the position of this helix is as in D_1, D_2, and D_3, but starts at the amino terminus of the polypeptide chain instead of residue 7. The major difference between the open procapsid (assumed to be a true assembly intermediate) and the closed procapsid (thought to be an assembly dead-end product) are the 30 Å diameter pores along the 3-fold axes of the open procapsid (Bernal et al., 2003; Dokland et al., 1999). These pores are closed by the 3-fold-related α4 helices of the F protein. Chimeric ϕX174 external scaffolding proteins in which the wild-type helix α1 has been replaced with the homologous helix from other *Microviridae* bacteriophages cannot assemble structural proteins into either procapsids or aberrant large particles (Burch and Fane, 2003). However, productive morphogenesis can be restored by introducing amino acid substitutions in helix α4 of the capsid protein (A. Uchiyama and B.A.F., unpublished data). These results suggest these two helices interact to initiate coat-scaffolding protein interactions and, perhaps, maintain open pores at the 3-fold axes of symmetry. Such an interaction would most likely be with helix α1 of D_4, which is closest to the icosahedral 3-fold axes of symmetry in the atomic structure of the closed procapsid.

Loop 5 in the D Protein

Loop 5 is the most polymorphic feature in the closed procapsid structure. In the D_A subunit, equivalent to D_1 and D_3 in the procapsid, loop 5 is an α helix, whereas in the D_B subunit, equivalent to D_2 and D_4, loop 5 is entirely disordered. However, loop 5 has a β structure in D_2. Thus, apparently, when the D tetramers bind to 12S particles, loop 5 becomes ordered in D_2 (but not in D_4), creating a surface in the 18S particles that is suitable for dimerization across 2-fold axes to form the open procapsid.

The Assembly Pathway

The results discussed above suggest that initially monomers of D associate to create asymmetric dimers similar to D_AD_B, as seen in the crystal structure of the recombinant D protein. The dimerization process involves either the kinking or unkinking of helix α3, depending on the nature of the unknown assembly naive monomer structure. The next step of assembly is the association of two dimers to make a tetramer. This results in further small conformational changes that inhibit the formation

Table 2. Data Collection and Refinement Statistics

Data Collection	
Resolution limit (Å)	3.3
Unique reflections	11,430
Completeness (%)[a,b]	94.2 (84.4)
$I/\sigma(I)$[a,b]	11.2 (2.3)
R_{sym}[a,b]	16.3 (52.4)
Refinement	
R_{cryst}[b]	27.1
R_{free}[b]	30.9
Rms deviation	
Bond lengths (Å)	0.009
Bond angles (°)	1.4
Dihedral angles (°)	20.4
Improper angles (°)	0.85
Average B factors	22.4

[a] Numbers in parentheses are for the highest resolution range.
[b] Completeness, $I/\sigma(I)$, R_{sym}, R_{cryst}, and R_{free} were computed over all observed reflections.

of infinite helices of D monomers or D_AD_B dimers. These tetramers then bind to 12S pentamers to create 18S particles. At this stage, helices α1 and α7 of subunit D_4 change their conformation as a result of their interaction with the F protein, thus anchoring the tetramer via subunit D_4 onto a capsid protein F and via subunit D_1 onto a spike protein G. Binding of the D tetramer with the 12S subunit activates a final conformational switch in which loop 5 of subunit D_2 becomes ordered, while loop 5 in subunit D_4 remains disordered, allowing 12 18S particles to assemble into an icosahedral open procapsid. Details of these events require further analyses, but the combination of structural and genetic analyses suggest the above as the approximate series of conformational switches that occur in ϕX174 procapsid assembly.

A general observation regarding protein structure is that the association of one protein with another, or with a smaller nonprotein ligand, usually increases the order and stability (James and Tawfik, 2003). The most disordered D subunit in the crystals of recombinant D is D_B, corresponding to D_2 and D_4 in the procapsid. This would suggest that D_B might be the closest to an assembly naïve structure.

Experimental Procedures

Protein Expression and Purification

Cloning of the ϕX174 D protein has been described previously (Burch and Fane, 2000). Recombinant D protein was overexpressed in *E. coli* BL21(DE3) cells. These cells were grown in LB media containing 100 mg/l ampicillin at 37°C. Overexpression was induced by addition of IPTG (isopropyl-β-D-thiogalactopyranoside) to a final concentration of 1 mM. The cell pellet from 350 ml of cultured cells was resuspended in 23 ml of 20 mM Tris-HCl, pH 8.0. Cells were lysed by sonication (Branson, Sonifier) for a total of 12 min, and the cellular debris removed by centrifugation at 15,000 $\times$ g for 20 min. After separation of the pellet and supernatant, 300 μl of 5 M NaCl was added to the supernatant, and the solution stirred for 15 min. Two grams of $(NH_4)_2SO_4$ were then added to the solution, followed by brief stirring. Another gram of $(NH_4)_2SO_4$ was then added and the solution stirred for an additional 15 min. The solution was then centrifuged at 15,000 $\times$ g for 20 min. The supernatant was removed, and the pellet was resuspended in 7 ml of 20 mM Tris-HCl, pH 8.0, and loaded onto a Q-Sepharose ion-exchange column (Amersham). Protein was eluted using a 0.0–1.0 M NaCl gradient in a 20 mM Tris-HCl, pH 8.0, buffer. D protein eluted at approximately 0.4 M NaCl. The eluted fractions were pooled, applied to a Superdex 200 (16/60) gel-filtration column (Amersham), and eluted with 20 mM Tris-HCl, pH 8.0, 50 mM NaCl. The single peak elution profile, calibrated with several standard proteins, corresponded to a molecular weight of 67 kDa (data not shown), showing that the 16 kDa D protein monomers had associated into tetramers. Sedimentation velocity and equilibrium analyses of the D protein showed an equilibrium between dimers and tetramers with the equilibrium shifting toward tetramers with increasing concentration of the D protein (unpublished data). The purified D protein was concentrated to 6 mg/ml using an Amicon Ultra Filtration Device (Millipore) and stored for approximately three weeks at 4°C before crystallization.

Crystallization, Data Collection, and X-Ray Structure Determination

D protein was crystallized using the hanging-drop vapor diffusion method. The protein crystallized in several different conditions available in Hampton Research sparse-matrix crystallization screens I and II. Crystal growth typically occurred within a few hours to a few days. Crystals used for X-ray diffraction data collection were grown in 8% PEG mono-methyl ether (MME) 5500 and 20 mM $(NH_4)_2SO_4$. These crystals were typically rod shaped, with dimensions of 0.2 $\times$ 0.03 $\times$ 0.02 mm.

Prior to data collection, crystals were briefly soaked in a cryo solution consisting of 8% (v/v) PEG MME 5500, 20 mM $(NH_4)_2SO_4$, and 10% (v/v) glycerol, and then frozen in liquid nitrogen. Cryo conditions were maintained during data collection with a stream of nitrogen gas cooled to 100 K. A 3.2 Å diffraction data set using the crystals of D protein was collected at the Advanced Photon Source (APS) 14BMc beam line using a Quantum Q4 CCD detector. The data were indexed, reduced, scaled, and merged using the programs HKL2000 and SCALEPACK (Otwinowski and Minor, 1997). The crystals are tetragonal, with space group $P4_12_12$, and unit cell parameters a = b = 106.44, c = 127.02 Å. The overall R_{sym} was 16.3% (Table 2). Similar values for R_{sym} were obtained when the data were indexed in lower symmetry space groups, indicating that the high R_{sym} value reflects the poor quality of the data rather than incorrect space group assignment. Two copies of the D_3 protein monomer, obtained from the closed procapsid structure (Dokland et al., 1999) (PDB accession number 1CD3), were positioned in the unit cell using the molecular replacement method (Rossmann, 1990), as implemented by the program AMoRe (Navaza, 1994). The program CNS (Brünger et al., 1998) was used for automated refinement (Table 2). The graphics program O (Jones et al., 1991) was used for manual model building. Water molecules were not added due to the low resolution of the data. The final $R_{working}$ and R_{free} values were 27.1% and 30.9%, respectively. This rather high crystallographic R factor is consistent with the low resolution and poor quality of the data (Table 2). There were 0 out of a total of 271 residues outside the allowed region of the Ramachandran plot.

Acknowledgments

We thank Cheryl Towell and Sharon Wilder for help in the preparation of this manuscript, and Susan Hafenstein and Asako Uchiyama for helpful discussions. The research was supported by NSF grants #MCB9986266 and #0234976 to M.G.R. and B.A.F., respectively, and an NIH postdoctoral fellowship 1F32 AI49683 to M.C.M.

Received: May 10, 2004
Revised: July 6, 2004
Accepted: July 14, 2004
Published: September 23, 2004

References

Berget, P. (1985). Pathways in viral morphogenesis. In Virus Structure and Assembly, S. Casjens, ed. (Boston: Jones and Bartlett), pp. 149–168.

Bernal, R.A., Hafenstein, S., Olson, N.H., Bowman, V.D., Chipman,

P.R., Baker, T.S., Fane, B.A., and Rossmann, M.G. (2003). Structural studies of bacteriophage α3 assembly. J. Mol. Biol. *325*, 11–24.

Brünger, A.T., Adams, P.D., Clore, G.M., DeLano, W.L., Gros, P., Grosse-Kunstleve, R.W., Jiang, J.S., Kuszewski, J., Nilges, M., Pannu, N.S., et al. (1998). Crystallography and NMR system: a new software suite for macromolecular structure determination. Acta Crystallogr. D Biol Crystallogr. *54*, 905–921.

Burch, A.D., and Fane, B.A. (2000). Foreign and chimeric external scaffolding proteins as inhibitors of *Microviridae* morphogenesis. J. Virol. *74*, 9347–9352.

Burch, A.D., and Fane, B.A. (2003). Genetic analyses of putative conformation switching and cross-species inhibitory domains in *Microviridae* external scaffolding proteins. Virology *310*, 64–71.

Casjens, S., and Hendrix, R. (1988). Control mechanisms in dsDNA bacteriophage assembly. In The Bacteriophages, R. Calendar, ed. (New York: Plenum Press), pp. 15–75.

Caspar, D.L.D. (1980). Movement and self-control in protein assemblies. Quasi-equivalence revisited. Biophys. J. *32*, 103–138.

Caspar, D.L.D., and Klug, A. (1962). Physical principles in the construction of regular viruses. Cold Spring Harb. Symp. Quant. Biol. *27*, 1–24.

Dokland, T. (1999). Scaffolding proteins and their role in viral assembly. Cell. Mol. Life Sci. *56*, 580–603.

Dokland, T., McKenna, R., Ilag, L.L., Bowman, B.R., Incardona, N.L., Fane, B.A., and Rossmann, M.G. (1997). Structure of a viral procapsid with molecular scaffolding. Nature *389*, 308–313.

Dokland, T., Bernal, R.A., Burch, A., Pletnev, S., Fane, B.A., and Rossmann, M.G. (1999). The role of scaffolding proteins in the assembly of the small, single-stranded DNA virus ϕX174. J. Mol. Biol. *288*, 595–608.

Fane, B.A., and Hayashi, M. (1991). Second-site suppressors of a cold-sensitive prohead assembly protein of bacteriophage ϕX174. Genetics *128*, 663–671.

Fane, B.A., and Prevelige, P.E., Jr. (2003). Mechanism of scaffolding-assisted viral assembly. Adv. Protein Chem. *64*, 259–299.

Farber, M.B. (1976). Purification and properties of bacteriophage ϕX174 gene D products. J. Virol. *17*, 1027–1037.

Fujisawa, H., and Hayashi, M. (1977). Assembly of bacteriophage ϕX174: identification of a virion capsid precursor and proposal of a model for the functions of bacteriophage gene products during morphogenesis. J. Virol. *24*, 303–313.

Hayashi, M., Aoyama, A., Richardson, D.L., Jr., and Hayashi, M.N. (1988). Biology of the bacteriophage ϕX174. In The Bacteriophages, R. Calendar, ed. (New York and London: Plenum Press), pp. 1–71.

James, L.C., and Tawfik, D.S. (2003). Conformational diversity and protein evolution: a 60-year-old hypothesis revisited. Trends Biochem. Sci. *28*, 361–368.

Jones, T.A., Zou, J.Y., Cowan, S.W., and Kjeldgaard, M. (1991). Improved methods for building protein models in electron density maps and the location of errors in these models. Acta Crystallogr. A *47*, 110–119.

King, J., and Casjens, S. (1974). Catalytic head assembling protein in virus morphogenesis. Nature *251*, 112–119.

King, J., Griffin-Shea, R., and Fuller, M.T. (1980). Scaffolding proteins and the genetic control of virus shell assembly. Q. Rev. Biol. *55*, 369–393.

Morais, M.C., Kanamaru, S., Badasso, M.O., Koti, J.S., Owen, B.A.L., McMurray, C.T., Anderson, D.L., and Rossmann, M.G. (2003). Bacteriophage ϕ29 scaffolding protein gp7 before and after prohead assembly. Nat. Struct. Biol. *10*, 572–576.

Navaza, J. (1994). AMoRe: an automated package for molecular replacement. Acta Crystallogr. A *50*, 157–163.

Otwinowski, Z., and Minor, W. (1997). Processing of X-ray diffraction data collected in oscillation mode. Methods Enzymol. *276*, 307–326.

Ray, P., and Murialdo, H. (1975). The role of gene Nu3 in bacteriophage lambda head morphogenesis. Virology *64*, 247–263.

Rossmann, M.G. (1990). The molecular replacement method. Acta Crystallogr. A *46*, 73–82.

Showe, M.K., and Black, L.W. (1973). Assembly core of bacteriophage T4: an intermediate in head formation. Nat. New Biol. *242*, 70–75.

Siden, E.J., and Hayashi, M. (1974). Role of the gene *B* product in bacteriophage ϕX174 development. J. Mol. Biol. *89*, 1–16.

Sun, Y., Parker, M.H., Weigele, P., Casjens, S., Prevelige, P.E., Jr., and Krishna, N.R. (2000). Structure of the coat protein-binding domain of the scaffolding protein from a double-stranded DNA virus. J. Mol. Biol. *297*, 1195–1202.

Thuman-Commike, P.A., Greene, B., Jakana, J., McGough, A., Prevelige, P.E., Jr., and Chiu, W. (2000). Interactions in a bacteriophage P22 mutant defective in maturation. J. Virol. *74*, 3871–3873.

Tonegawa, S., and Hayashi, M. (1970). Intermediates in the assembly of ϕX174. J. Mol. Biol. *48*, 219–242.

Wood, W.B., and Conley, M.P. (1979). Attachment of tail fibers in bacteriophage T4 assembly. J. Mol. Biol. *127*, 15–29.

Accession Numbers

Coordinates and structure factors have been deposited with the Protein Data Bank (accession number 1TX9).